

6-*O*-(2-[¹⁸F]Fluoroethyl)-6-*O*-Desmethyldiprenorphine ([¹⁸F]DPN): Synthesis, Biologic Evaluation, and Comparison with [¹¹C]DPN in Humans

Hans-J. Wester, Frode Willoch, Thomas R. Tölle, Frank Munz, Michael Herz, Ivar Øye, Jan Schadrack, Markus Schwaiger, and Peter Bartenstein

Departments of Nuclear Medicine and Neurology, Technische Universität München, Munich; Max-Planck Institute of Psychiatry, Munich, Germany; and Department of Pharmacology, University of Oslo, Oslo, Norway

6-*O*-(2-[¹⁸F]fluoroethyl)-6-*O*-desmethyldiprenorphine ([¹⁸F]DPN) was developed and biologically evaluated. Results of animal experiments, binding studies in vivo, and a human PET study are reported and compared with those of [¹¹C]DPN. **Methods:** [¹⁸F]DPN was obtained by ¹⁸F-fluoroethylation of 3-*O*-trityl-6-*O*-desmethyldiprenorphine and subsequent deprotection in good radiochemical yields (23% ± 7%; 100 min; 37 TBq/mmol). Binding of [¹⁸F]DPN to μ, κ, and δ opioid receptors was shown by autoradiography studies on rat brain slices. Quantification of cerebral opioid receptor binding in men was performed by spectral analysis of a dynamic PET scan (25 frames, 90 min) after intravenous application of 63 MBq [¹⁸F]DPN (36 GBq/μmol) and correction for metabolites. **Results:** [¹⁸F]DPN shows high affinity to opioid receptors. Parametric images (impulse response function at 60 min) of this human study showed a binding pattern of [¹⁸F]DPN equal to that of a control group (n = 9 healthy volunteers) after administration of [¹¹C]DPN. **Conclusion:** The advantage of the longer half-life of ¹⁸F will allow extended scanning periods, more flexible interventions (e.g., displacement studies), and DPN to be available to PET centers without an on-site cyclotron.

Key Words: diprenorphine; ¹⁸F; PET; opioids; [¹⁸F]DPN

J Nucl Med 2000; 41:1279–1286

The opioid receptor system plays a major role in pain modulation (1) and various pathologic processes, including addiction (2), neurodegeneration (3), and epilepsy (4). Changes observed in these processes involved either all receptor subtypes or a combination of μ, κ, and δ receptors. Thus, extensive research efforts have been directed toward the identification and characterization of radioligands suitable for localization and quantification of opioid receptors by PET. Various ligands with different specificities were evaluated, such as [¹¹C]carfentanil (μ) (4–6), [¹¹C]buprenorphine (μ and κ) (7–10), *N*-1'-([¹¹C]methyl)naltrindole (δ) (11–13), 3-[¹⁸F]acetylcyclofoxy (μ) (14,15), and

[¹⁸F]cyclofoxy (μ and κ) (16,17). Because of its favorable pharmacologic properties, [¹¹C]diprenorphine (9,18–20), a nonsubtype-selective opioid antagonist with subnanomolar affinity, is currently the most widely used ligand for PET studies of the opioid receptor system (1,3,21–26).

Attempts to determine the central release of endogenous opioids by displacement of [¹¹C]diprenorphine in vivo using PET are complicated by the short half-life (*t*_{1/2}) of ¹¹C (*t*_{1/2} = 20.4 min). As a consequence of the low activity at the end of the scanning procedure, the sensitivity for small signal changes is limited (21). ¹⁸F labeling of diprenorphine (*t*_{1/2} = 110 min) can improve signal intensity and, thus, statistics and accuracy of these investigations and make this tracer available for PET satellite systems. ¹⁸F-labeled derivatives of diprenorphine and buprenorphine have been synthesized by *N*-[¹⁸F]fluoroalkylation of nordiprenorphine and norbuprenorphine (27–29) (Fig. 1). Compared with the parent compounds, *N*-(3-[¹⁸F]fluoropropyl)-*N*-norbuprenorphine and *N*-(3-[¹⁸F]fluoropropyl)-*N*-nordiprenorphine were less potent in vivo and decreased rapidly in receptor-rich brain structures (28). Furthermore, baboon studies showed that the appearance of metabolites in plasma was rapid, with >90% present at 10 min after injection (27).

Consequently, we examined an alternative ¹⁸F-labeling methodology through ¹⁸F-fluoroethylation of the 6-hydroxy position (Fig. 1) and describe the synthesis and in vivo evaluation of 6-*O*-(2-[¹⁸F]fluoroethyl)-6-*O*-desmethyldiprenorphine ([¹⁸F]DPN). Quantitative results of this human study, using spectral analysis according to Cunningham and Jones (30), are compared with data obtained with [¹¹C]DPN.

MATERIALS AND METHODS

Chemicals

Kryptofix and acetonitrile (MeCN; for DNA syntheses) were obtained from Merck (Darmstadt, Germany). Triphenylmethylchloride (Trt-Cl) was purchased from Sigma Chemikalien (Taufkirchen, Germany). DPN was obtained from Macfarlan Smith Ltd. (Edinburgh, England). [3-*O*-Trityl-6-*O*-desmethyl]diprenorphine (TDD) was purchased from ABX Biochemicals (Dresden,

Received May 6, 1999; revision accepted Nov. 1, 1999.
For correspondence or reprints contact: Hans-J. Wester, PhD, Department of Nuclear Medicine, Technische Universität München, Ismaningerstr. 22, 81675 München, Germany.

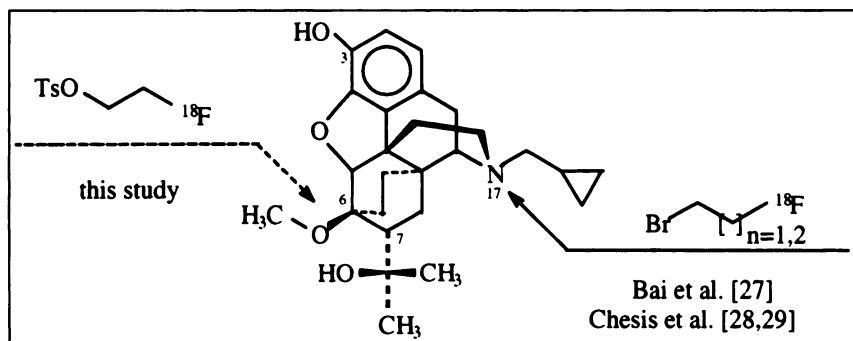


FIGURE 1. Approaches to [¹⁸F]DPN.

Germany). All other reagents were purchased from Aldrich (Deisenhofen, Germany) without further purification.

Synthesis of [¹⁸F]DPN

After TDD (117 mg, 0.18 mmol) was dissolved in 5 mL dimethylformamide (DMF), dry sodium hydride (41.1 mg, 1.79 mmol) was added, and the reaction mixture was stirred for 5 min before addition of 2-fluoroethyltosylate (39.3 mg, 0.18 mmol) (31) in 1 mL DMF. After stirring for 90 min at ambient temperature, the temperature was increased to 90°C and HCl (8 mL, 2 mol/L) was added. After 10 min, the reaction mixture was cooled and neutralized with aqueous NaOH (2 mol/L). The solution was rotary evaporated to dryness, and the residue was extracted with MeCN (2 × 3 mL). After the solvent was removed, the residue was purified by preparative high-performance liquid chromatography (HPLC) (Multospher RP₁₈, 250 × 20 mm; CS-Chromatographie Service, Langerwehe, Germany) eluted at 3 mL/min with methanol/0.1N ammonium formate (75:25, volume/volume). The mass (457.58) and structure were confirmed on the LC-MS system LCQ from Finnigan (Bremen, Germany) and by nuclear magnetic resonance, respectively.

Synthesis of [¹⁸F]DPN

[¹⁸F]DPN was prepared by a 3-step reaction, which consisted of ¹⁸F-fluorination of ethylene glycol-1,2-ditosylate (31), ¹⁸F-fluoroethylation of TDD, and final acidic deprotection of the product. [¹⁸F]fluoride was produced through the ¹⁸O(*p,n*)¹⁸F nuclear reaction. The aqueous [¹⁸F]fluoride solution (0.35 mL) was added to a 2.5-mL conical vial containing 0.25 mL dry MeCN, 5 mg (13.3 μmol) Kryptofix 2.2.2, and 5 μL 1 mol/L potassium carbonate (Merck; suprapure). The solvent was evaporated under a stream of nitrogen at 90°C. Azeotropic drying was repeated at least twice (depending on the amount of target water) with 250-μL portions of MeCN. Five milligrams (12 μmol) ethylene glycol-1,2-ditosylate in 300 μL MeCN were added to the dried kryptate (K⁺ C 2.2.2) ¹⁸F⁻ and heated at 90°C for 10 min. ¹⁸F-fluoroethyltosylate was purified by reversed-phase HPLC (RP-HPLC) (LiChrosorb RP-select B (CS-Chromatographie Service), 125 × 8 mm; CH₃CN/H₂O [50:50, volume/volume], 4 mL/min, capacity factor [k'] = 5.7; preparative radiochemical yield, 65% ± 5%). After on-line fixation of the product fraction on a polystyrene cartridge (LiChrolut EN; Merck) and drying of the cartridge with nitrogen, the product was eluted with 0.9 mL MeCN. The solvent was removed, and the residue was redissolved in 300 μL DMF containing TDD (2 mg, 3.1 μmol) and dry sodium hydride (4.5 mg, 0.187 mmol). After the mixture was stirred for 5 min at 100°C, 300 μL HCl (2N) were added and heated for an additional 2 min. The reaction mixture was cooled to about 40°C and diluted with 5 mL aqueous ammonia (20%). Because of the large sample volume, HPLC purification was performed by the

trace enrichment technique. The solution was loaded into an injection loop (6 mL) and transferred onto a sample enrichment column (30 × 20 mm) packed with polystyrene-divinylbenzene. The enrichment column was washed at a flow rate of 2.75 mL/min for 4 min and then eluted in the reverse direction onto a semipreparative column (μBondapak C₁₈, 30 × 0.78 cm inner diameter; CS-Chromatographie Service) using the mobile phase, MeCN/0.1N ammonium formate (55:45, volume/volume), at a flow rate of 3 mL/min. The mobile phase was monitored continuously for both radioactivity and ultraviolet absorbance (254 nm). The product fraction eluting between 9 and 10.5 min was pumped into a rotary evaporation flask containing 1% 2 mol/L HCl in ethanol (1 mL) and evaporated to dryness under reduced pressure. The radioactive product was then formulated for injection by dissolving in isotonic saline (10 mL, 0.9% NaCl) and transferring through a Millipore filter (Millex GS, 0.22 μm; Millipore, Inc., Bedford, MA) into a sterile vial containing bicarbonate (100 μL, 8.4% [volume/weight]). The pH of the formulated solutions was about 7. Quality control was performed by HPLC (LiChrolut RP₁₈, 250 × 4 mm; MeOH/0.1N ammonium formate (70:30, volume/volume) (1 mL/min; k' = 3.5). The 3-step radiosynthesis delivers [¹⁸F]DPN in ~100 min with a radiochemical yield of 22% ± 7%, a radiochemical purity of >98%, and a specific activity of 37 TBq/mmol.

Synthesis of [6-O-methyl-¹¹C]Diprenorphine

The synthesis was performed according to Luthra et al. (9). The radiosynthesis typically delivers 1.2–2.5 GBq [¹¹C]DPN with a radiochemical purity of >96% and a specific activity of 4–36 TBq/mmol (time of injection) in about 40–50 min from the end of bombardment. Quality control was performed by HPLC (LiChrolut RP₁₈, 250 × 4 mm; MeOH/0.1N ammonium formate (70:30, volume/volume) (1 mL/min; k' = 3.1).

Animal Experiments

Tissue Distribution of [¹⁸F]DPN and [¹¹C]DPN in Mice. Female mice, weighing ~25 g, were injected in the lateral tail vein with 7.4–25.9 MBq [¹¹C]DPN or 185 MBq [¹⁸F]DPN. The mice injected with [¹¹C]DPN were killed by cervical dislocation at 5, 10, and 60 min after injection; the time points for mice injected with [¹⁸F]DPN were 5, 10, 30, 60, 120, and 240 min after injection. The radioactivity of each weighed tissue sample was measured in a γ-counter. Data are expressed as percent injected dose per gram tissue (%ID/g) and percent injected dose per organ (%ID/organ) (n = 4, unless stated otherwise; mean ± SD).

Extrapolated Human Dose Calculations for [¹⁸F]DPN. Cumulative activities and residence times in all organs were calculated from the biodistribution data obtained in mice. Dose calculations

were performed using the program MIRDOSE3 according to the guidelines outlined by the MIRDO Committee (32).

Mice Plasma and Brain Metabolite Analysis. Female mice were injected with 25.9 MBq [¹¹C]DPN (n = 2) or 7.4 MBq [¹⁸F]DPN (n = 2) and killed 30 min after injection. For studies on the cerebral metabolism, brain tissue homogenates were prepared immediately after dissection by mechanical homogenization of nitrogen-frozen tissue samples and spiked with unlabeled DPN by addition of 1 mL isotonic saline solution and 100 μL 1 μmol/L DPN. The mixture was vigorously vortexed. After 2 mL MeCN were added, the samples were centrifuged for 5 min at 12,000g. To determine the amount of unchanged tracer, the supernatants were analyzed by HPLC. Analysis was based on the fraction unchanged as determined by HPLC.

Autoradiography of In Vivo Binding. A comparison of the in vivo binding properties of [¹⁸F]DPN and [³H]DPN was performed by autoradiographic techniques. Thirty-seven megabecquerels [¹⁸F]DPN and 2.96 MBq [³H]DPN were coinjected subcutaneously in 4 Sprague-Dawley rats. The rats were decapitated 60 min after injection, and the brains were rapidly excised, frozen, and sectioned into 60-μm-thick slices. Autoradiography was performed by exposing the sections on a phosphor screen; [¹⁸F]DPN was exposed for 6 h. After complete decay of the ¹⁸F ligand, [³H]DPN was exposed for 3 wk. Analyses were performed using a digital phosphor imaging device. Nonspecific binding was determined in 2 of the rats by pretreatment with naloxon (1 mg/kg).

Autoradiography of In Vitro Binding. To identify potential receptor subtype selectivity, the binding pattern of [¹⁸F]DPN on rat brain slices was compared with subtype-selective ligands. For this purpose, autoradiography was performed using unfixed frozen sections (20 μm) on adjacent sections. After thawing and drying, sections were preincubated in 15 mmol/L Tris-HCl buffer (pH 7.4) for 30 min and incubated for 1 h at room temperature in 50 mmol/L Tris-HCl buffer (pH 7.4) containing 4.2 nmol/L ³H-[D-Ala²,N-Me-Phe⁴,Gly-ol⁵]enkephalin (DAMGO; Biotrend Chemikalien GmbH, Cologne, Germany) (³H-DAMGO; Amersham Pharmacia Biotech, Freiburg, Germany) (μ binding), 7.6 nmol/L ³H-((+)-(5α,7α,8β)-N-methyl-N-[7-(1-pyrrolidinyl)-1-oxaspiro[4,5]dec-8-yl]benzeneacetamide) (U69,593; Biotrend Chemikalien) (³H-U69,593; Amersham Pharmacia Biotech) (κ binding), or 14.4 nmol/L ³H-[D-Pen²⁻⁵]enkephalin (DPDPE; Biotrend Chemikalien) (³H-DPDPE; NEN DuPont International, Wilmington, DE) (δ binding). After the sections were washed twice in 50 mmol/L Tris-HCl at 4°C for 3 min, they were dipped in distilled H₂O at 4°C. For saturation binding, the concentrations of the radioligands used corresponded to approximately twice their dissociation constant values. Nonspecific binding was determined in the presence of excess unlabeled ligands: 4.2 μmol/L DAMGO, 7.6 μmol/L U69,593, or 14.4 μmol/L DPDPE. All sections were exposed to ³H-Hyperfilm (Amersham Pharmacia Biotech) for 10 wk.

Human Studies

Subjects. The data obtained from the volunteer (male; age, 36 y) after administration of [¹⁸F]DPN were compared with [¹¹C]DPN studies in 9 healthy volunteers (men; mean age, 37 y; age range, 23–67 y) performed previously in our institution. None of the volunteers had a previous history of severe internal or neurological diseases, and a brief neurological investigation revealed no abnormalities. None of the volunteers had a constant use of medications with central nervous system effects or had consumed medications with central nervous system effects for at least 1 mo before participation. All subjects gave informed written consent. The

studies were approved by the ethics committee of medicine of the Technische Universität München and the radiation protection authorities.

Data Acquisition. PET studies were performed on an ECAT EXACT scanner (CTI/Siemens, Knoxville, TN) in 2-dimensional mode with a total axial field of view of 16.2 cm. Attenuation was corrected using a transmission scan performed before injection. After intravenous administration of 63 MBq [¹⁸F]DPN, a dynamic PET scan was acquired over 90 min with a total of 25 frames ranging from 30 s to 90 min (23). The arterial input function corrected for metabolites was calculated from approximately 60 arterial samples. The data of the 9 control subjects were acquired using the same protocol with a median [¹¹C]DPN activity of 630 MBq (range, 160–740 MBq). All datasets were reconstructed by filtered backprojection with a ramp filter (cutoff, 0.3 cycle/projection element), with 2-dimensional smoothing, and without decay correction.

Metabolite Analysis. For quantification of unchanged tracer in human plasma, metabolite analyses were performed. For this purpose, blood samples of 8 mL were taken 2, 5, 10, 25, and 45 min after injection of [¹¹C]DPN or [¹⁸F]DPN and centrifuged at 3200g for 3 min. Samples of the supernatant plasma (2 mL) were passed through SepPak RP₁₈ cartridges (Waters Corp., Milford, MA). The cartridges were washed with 10 mL 0.1 mol/L ammonium formate. To calculate the radioactivity balance and extraction efficiency, the radioactivity of the combined liquids from the fixation and the washing step and the radioactivity of the extracted material were measured in a γ-counter. Elution of radiolabeled DPN from the cartridges was performed with 1.5 mL MeOH at a flow rate of 0.75 mL/min. The radioactivity balance and efficiency of this step were determined as described. Finally, the prepared samples were diluted with 0.5 mL 0.1 mol/L ammonium formate and analyzed by HPLC (LiChrospher, 125 × 8 mm; methanol/0.1 mol/L ammonium formate [65:35; volume/volume]; flow rate, 3.5 mL/min; 500-μL samples). The amount of unchanged ligand in the plasma (T_{p,u}) (%) was calculated using the following equation:

$$T_{p,u} = [F_T / (F_T + F_M)] \times E_F \times E_E \times E_R \times (1/10,000),$$

where F_M is the fraction of metabolites (%) determined by HPLC, F_T is the fraction of unchanged tracer (%) determined by HPLC, E_F is the efficiency (%) of the plasma extraction step, E_E is the efficiency (%) of the cartridge elution procedure, and E_R represents the recovery of activity from HPLC.

Plasma Protein Binding of Radiolabeled DPN. Determination of plasma protein binding at 45 min after injection of radiolabeled DPN was carried out by ultrafiltration as described (26).

Data Analysis. Parallel spectral analysis (30) was applied on a voxel level to directly compare the distribution of [¹¹C]DPN and [¹⁸F]DPN without any a priori assumptions. On the basis of an F test (P < 0.001), noise-related peaks in the kinetic spectra were suppressed (33). A K₁ image (unidirectional clearance of the tracer from plasma to tissue (mL/min × mL tissue) was calculated from the value of the unit impulse response function (IRF) at time = 1 min (30).

The direct calculation of the total volume of distribution (VD) relative to the arterial plasma for every voxel is sensitive to noise in the time–activity curves. Therefore, we determined the value of the IRF at time = 60 min (IRF₆₀), which is numerically more stable and highly correlated with the VD (33). Values were assessed by a volume-of-interest (VOI) analysis, each 1.6-cm diameter, in the non-normalized images using a predefined set of 78 VOIs covering

the equivalent areas that were adapted to the individual brain. Data from VOIs within predefined anatomic regions were averaged (23). Brain uptake kinetics were assessed over the occipital cortex as a measure of nonspecific binding (6,21,26), over the thalamus (predominantly μ), over the striatum (predominantly $\delta > \mu$), and over the medial prefrontal cortex (μ , $\delta \gg \kappa$). The derived kinetics were compared with the kinetics obtained with [^{11}C]DPN.

RESULTS

Synthesis of [^{18}F]DPN

The 3-step radiosynthesis delivers [^{18}F]DPN in ~ 100 min with a radiochemical yield of $22\% \pm 7\%$, a radiochemical purity of $>98\%$, and a specific activity of 37 TBq/mmol. The overall synthesis time consists of 40 min for the preparation of [^{18}F]fluoroethyltosylate, 40 min for ^{18}F -fluoroalkylation and subsequent deprotection, and about 20 min during which quality control is completed. Alkylation and deprotection were remotely controlled using a module for the routine production of [^{11}C]DPN according to Luthra et al. (9) with some modifications.

Tissue Distribution and Uptake Kinetics of [^{18}F]DPN

Tables 1 summarizes the tissue distribution data of [^{18}F]DPN and some reference data obtained with [^{11}C]DPN in mice. The brain uptake kinetics of [^{11}C]DPN is fast, with a high, but rapidly declining, activity accumulation (7.50 ± 0.89 %ID/g 7 min after injection). In contrast, [^{18}F]DPN shows a lower initial brain uptake maximum (4.36 ± 0.49 %ID/g 5 min after injection) and a slower brain clearance, leading to comparable uptake values for both compounds at longer observation times. Most ^{18}F activity is hepatobiliary cleared from the circulation with a kinetics somewhat slower than that of [^{11}C]DPN.

The uptake kinetics in bone after administration of [^{11}C]DPN and [^{18}F]DPN show comparable results up to 60 min after injection with continuously decreasing values. Thus, only the small increase of ^{18}F activity in the bones occurring between 60 (0.82 ± 0.11 %ID/g) and 240 min (1.51 ± 0.11 %ID/g) seems to represent trapping of free ^{18}F -fluoride (Table 1).

Dosimetric Calculations

Using the approximation that the biodistribution, kinetics, metabolism, distribution of metabolites, and resident times in humans are identical to those in mice, dosimetric calculations were performed by the MIRD procedure using the tissue uptake kinetics of [^{18}F]DPN in mice up to 240 min after injection to generate an estimate of the whole-body dose after administration of [^{18}F]DPN in humans (Table 2). Considering the above assumptions, for a reference adult an effective dose equivalent of 5.59×10^{-2} mSv/MBq and an effective dose of 5.10×10^{-2} mSv/MBq were calculated.

Mice Plasma and Brain Metabolite Analysis

In comparison with [^{11}C]DPN, [^{18}F]DPN showed a faster metabolization in mice. Thirty minutes after injection, 1 major peak corresponding to a hydrophilic metabolite was detected by HPLC and represented $>95\%$ of the ^{18}F activity present in plasma of mice (about 90% metabolization in plasma for [^{11}C]DPN at the same time point). More significant and important, quantification of metabolites in brain of mice differed for the 2 compounds. As reported by Sadzot et al. (26) and confirmed in this study, no labeled metabolites were detected in mice brain 30 min after administration of [^{11}C]DPN. In contrast, only 80% of the activity extracted from the brain of mice 30 min after injection of [^{18}F]DPN coeluted with the unlabeled standard. The metabolite fraction consisted mainly of a hydrophilic component with negligible retention under the chromatographic conditions used.

Autoradiography

Ex vivo autoradiographic studies of rat brain at 60 min after injection of 18.5 kBq [^{18}F]DPN showed similar distributions of [^3H]DPN and [^{18}F]DPN. In vivo competition revealed nearly complete displacement of [^{18}F]DPN (Fig. 2). The average ^{18}F activity of the cortex, striatum, and thalamus equaled the ^{18}F activity of the cerebellum, which is known to be devoid of opioid receptors in rats. Additionally, the binding patterns of ^3H -DAMGO, ^3H -DPDPE, and ^3H -U69,593 to rat brain opioid receptors are shown. Compared

TABLE 1
Biodistribution of [^{18}F]DPN and Uptake Kinetics of [^{11}C]DPN in Female Mice

Tissue	Biodistribution of [^{18}F]DPN (%ID/g)						Uptake kinetics of [^{11}C]DPN (%ID/g)			
	Time after injection (min)						Time after injection (min)			
	5 (n = 4)	10 (n = 4)	30 (n = 5)	60 (n = 4)	120 (n = 4)	240 (n = 4)	Tissue	7 (n = 3)	15 (n = 3)	60 (n = 3)
Blood	4.73 \pm 1.20	3.41 \pm 1.11	2.33 \pm 0.17	1.33 \pm 0.18	1.03 \pm 0.41	0.69 \pm 0.05	Blood	3.44 \pm 0.29	2.67 \pm 0.31	0.86 \pm 0.27
Bone	2.73 \pm 0.16	2.15 \pm 0.22	1.33 \pm 0.23	0.82 \pm 0.11	0.96 \pm 0.15	1.51 \pm 0.11	Bone	2.83 \pm 0.52	1.83 \pm 0.17	0.62 \pm 0.20
Brain	4.36 \pm 0.49	3.79 \pm 1.06	3.55 \pm 0.87	1.96 \pm 0.27	0.69 \pm 0.09	0.39 \pm 0.01	Brain	7.50 \pm 0.89	5.65 \pm 0.86	2.27 \pm 0.29
Kidney	18.1 \pm 3.0	10.5 \pm 1.8	7.34 \pm 1.40	2.22 \pm 0.40	0.96 \pm 0.13	0.71 \pm 0.05				
Intestine	10.3 \pm 2.4	10.9 \pm 2.7	16.8 \pm 2.6	27.5 \pm 2.4	30.7 \pm 1.6	36.85 \pm 2.60				
Muscle	4.00 \pm 1.62	2.1 \pm 0.8	1.88 \pm 0.36	1.01 \pm 0.61	0.28 \pm 0.03	0.22 \pm 0.06				
Liver	19.0 \pm 2.9	12.7 \pm 2.9	11.2 \pm 2.3	9.93 \pm 2.92	6.46 \pm 1.02	7.32 \pm 2.29				

All values are mean \pm SD.

TABLE 2
Radiation Dose Estimates for Reference Adult

Effective dose equivalent (5.59E-2 mSv/MBq)				Effective dose (5.10E-2 mSv/MBq)	
Tissue	mGy/MBq	Tissue	mGy/MBq	Tissue	mGy/MBq
Adrenals	6.07E-3	Kidneys	1.38E-2	Spleen	4.72E-3
Brain	3.04E-3	Liver	2.92E-2	Testes	6.48E-3
Breasts	1.34E-3	Lungs	2.52E-3	Thymus	1.57E-3
Gallbladder wall	2.07E-2	Muscle	7.82E-3	Thyroid	1.26E-3
LL intestine wall	1.70E-1	Ovaries	3.59E-2	Urinary bladder wall	1.97E-1
Small intestine	1.26E-1	Pancreas	7.49E-3	Uterus	3.10E-2
Stomach	9.47E-3	Red marrow	1.09E-2	Total body	9.86E-3
UL intestine wall	2.23E-1	Bone surface	1.03E-2		
Heart wall	2.90E-3	Skin	2.68E-3		

LL = lower large; UL = upper large.

Radiation dose estimates are based on biodistribution data and residence times as assessed in mice.

with these ligands, the [¹⁸F]DPN binding pattern resembles the distribution of at least μ and δ receptors, which are abundant in the structures covered by the slices used for imaging (Fig. 2). Because κ -receptor density is very low, the contribution of κ -receptor located [¹⁸F]DPN in the investigated structures is minimal.

Human Study

PET imaging with [¹⁸F]DPN was performed over a period of 90 min. ¹⁸F activity was highly accumulated and retained in opioid receptor-rich regions, such as thalamus, striatum, and medial prefrontal cortex (Fig. 3). The activity in the cerebellum, which has intermediate opioid receptor density, showed the expected faster decline (not shown). In the occipital cortex (very low opioid receptor density), the kinetics showed an even faster decline. Thus, the uptake kinetics of [¹⁸F]DPN resembles closely that of [¹¹C]DPN (Figs. 3 and 4), whereas the ¹⁸F activity in the occipital

cortex declined somewhat slower, probably because of a higher amount of nonspecific binding (Fig. 4B). However, the uptake ratios of the different cerebral regions at 80 min after injection, which can be used as a measure of binding potential, are very similar to the corresponding [¹¹C]DPN database (uptake ratios of [¹¹C]DPN database [n = 9; mean \pm SD] versus [¹⁸F]DPN: 3.17 \pm 0.40 versus 3.27 for thalamus/occipital cortex; 3.07 \pm 0.41 versus 2.90 for striatum/occipital cortex; and 2.56 \pm 0.23 versus 2.66 for medial prefrontal cortex/occipital cortex).

The recovery of radioactivity from the human arterial samples for [¹⁸F]DPN and [¹¹C]DPN was found to be nearly identical. The kinetics of nonmetabolized [¹⁸F]DPN, expressed as the fraction of unchanged ligand in plasma, show only a small difference in the decrease of unchanged tracer compared with the [¹¹C]DPN database. The small differences were within the error bars of the latter compound.

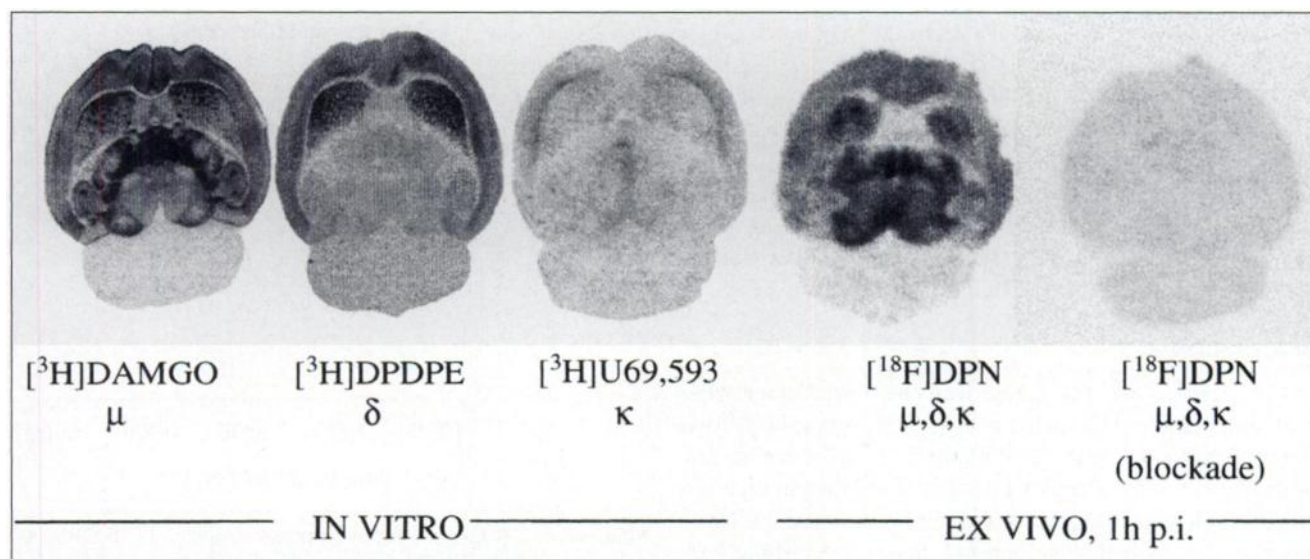


FIGURE 2. In vitro and ex vivo (1 h after injection) autoradiographs of opioid receptor sites in rat brain. Nonspecific binding was determined by pretreatment with naloxone (1 mg/kg). p.i. = postinjection.

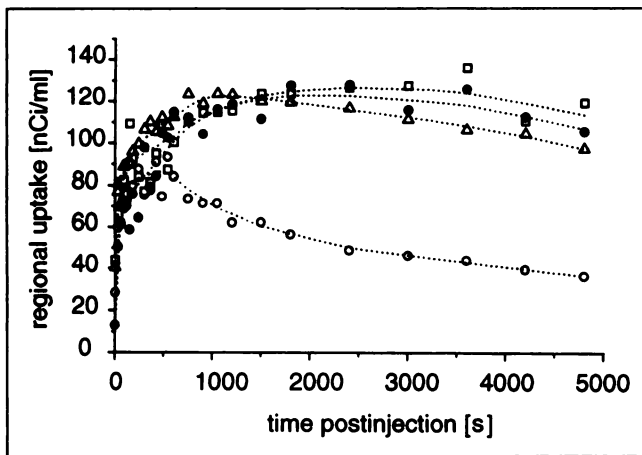


FIGURE 3. Human brain uptake kinetics of [^{18}F]DPN in striatum (●), occipital cortex (○), thalamus (□), and medial prefrontal cortex (△).

^{18}F -labeled metabolites appear soon after the intravenous injection of [^{18}F]DPN and consist mainly of a significantly more polar fraction under RP-HPLC conditions. Plasma protein binding of [^{18}F]DPN in humans was measured to be 0.78 ± 0.05 , thus being somewhat higher compared with [^{11}C]DPN (0.70 ± 0.03) (26). In agreement with the higher plasma protein binding of [^{18}F]DPN, the time course of the activity in human plasma revealed a slower clearance of the fluorinated tracer ($t_{1/2} = \sim 55$ min compared with 18 min).

Quantification of [^{18}F]DPN binding by means of spectral analysis revealed the same pattern on the K_1 image as that obtained with [^{11}C]DPN, reflecting regional cerebral blood flow. The IRF₆₀ image obtained by this approach reveals the expected opioid receptor distribution. Figure 5 illustrates the great similarities in the IRF₆₀ images of [^{11}C]DPN and [^{18}F]DPN.

It is noteworthy that the ^{18}F activity injected was only one sixth of the administered ^{11}C activity for this comparison. The quantitative values derived from the spectral analysis and the IRF₆₀ images are very similar for both compounds; the IRF₆₀ values for [^{18}F]DPN were found to be within the SD of the corresponding values for the [^{11}C]DPN database. The results for the medial prefrontal cortex were 0.16563 and 0.14703 ± 0.02996 , respectively; for the thalamus, 0.20290 and 0.16839 ± 0.04668 ; for the striatum, 0.18440 and 0.16101 ± 0.03251 ; and for the occipital cortex, 0.03435 and 0.03056 ± 0.01123 , respectively.

DISCUSSION

The purpose of this study was the development and evaluation of the ^{18}F -labeled analog of diprenorphine. Two former approaches to [^{18}F]DPN failed (27–29) because one of the most sensitive regions toward alterations in receptor binding with respect to affinity and selectivity was modified—namely, the *N*-methylcyclopropyl moiety. As shown by previous studies (34,35), morphine-6-glucuronide, one of the major metabolites of morphine metabolism, not only

crosses the blood–brain barrier (BBB) but also shows a 2- to 3-fold higher opioid receptor affinity and unaffected μ selectivity. Therefore, substitution of the methyl group at the oxygen at C_6 by a 2- ^{18}F fluoroethyl group seemed to be a promising approach.

The synthesis of [^{18}F]DPN consists of steps that are comparable with those described for the preparation of [^{11}C]DPN (9). Thus, adaptation was easily accomplished with the module used routinely for the large-scale production of [^{11}C]DPN. To avoid potential side reactions, such as *N*-alkylation and crosslinking (caused by the excess of bistyloxyethane in relation to [3-*O*-trityl-6-desmethyl]diprenorphine), a 1-pot strategy without intermediate purification of 2- ^{18}F fluoroethyltosylate was not tested.

The in vitro evaluation and animal experiments show that affinity and selectivity of [^{18}F]DPN to opioid receptors are comparable with those of [^{11}C]DPN. Small alterations in BBB permeability between methylated and the corresponding fluoroethylated compounds, as observed in this study, were also found in earlier studies (36,37). However, when longer PET protocols are needed, the small decline in brain uptake compared with [^{11}C]DPN is overcompensated by the longer $t_{1/2}$ of [^{18}F]DPN.

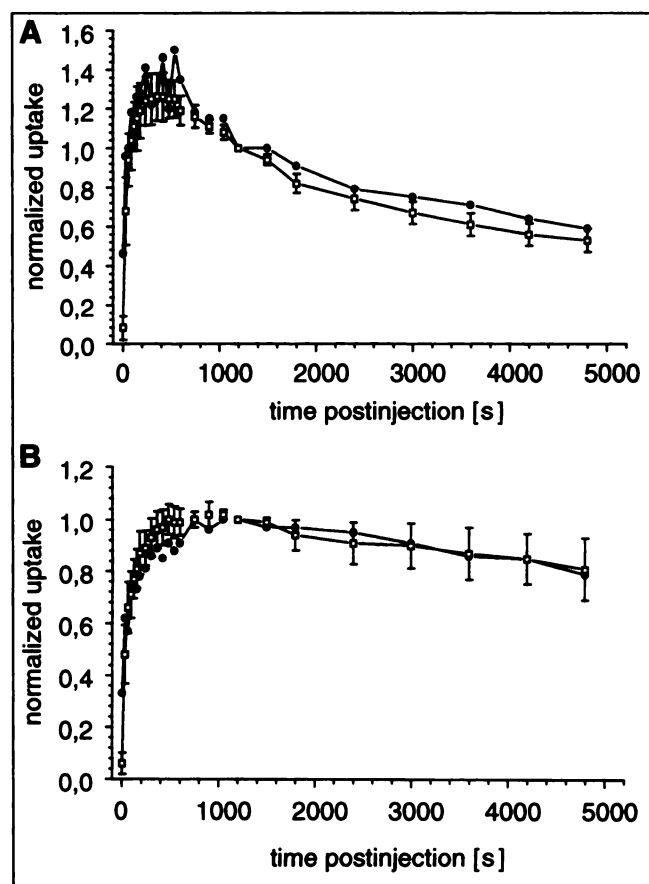


FIGURE 4. Regional cerebral uptake kinetics of [^{18}F]DPN (●) compared with [^{11}C]DPN database (□) ($n = 9$, mean \pm SD; SD is represented by error bars). (A) Occipital cortex. (B) Medial prefrontal cortex.

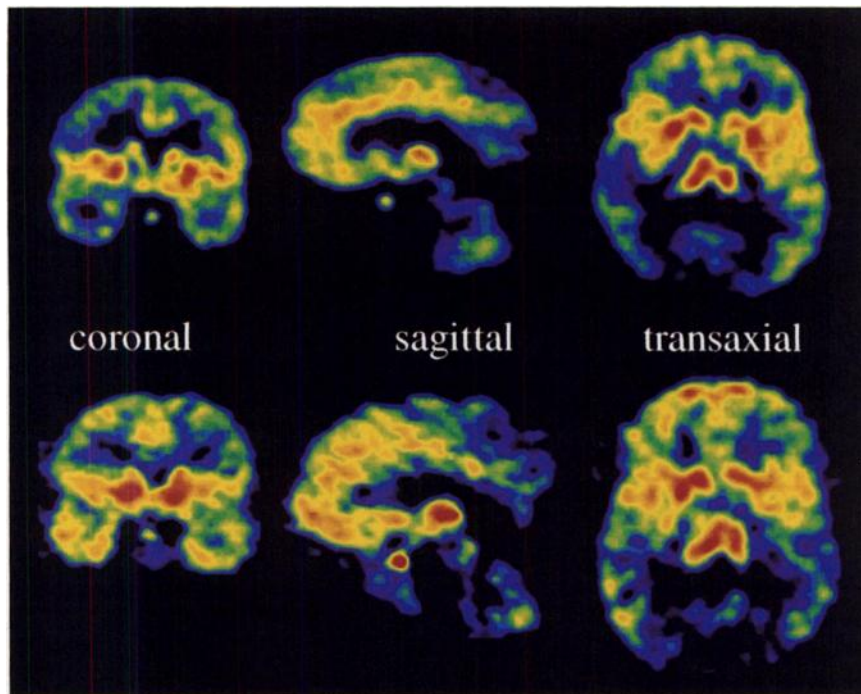


FIGURE 5. IRF₆₀ images of identical coronal, sagittal, and transaxial brain images of 2 healthy volunteers after application of 370 MBq [¹¹C]DPN (top row) and 63 MBq [¹⁸F]DPN (bottom row).

Using the estimates for the whole-body dose of [¹⁸F]DPN (5.10×10^{-2} mSv/MBq), about 185 MBq [¹⁸F]DPN give the same absorbed radiation dose caused by 370 MBq FDG. Thus, limiting the administered activity to about 185 MBq [¹⁸F]DPN, the remaining absolute body activity 50 min after injection is equal to that after an application of 740 MBq [¹¹C]DPN.

Compared with the [¹¹C]DPN normal database, the regional cerebral uptake kinetics and the data derived from this [¹⁸F]DPN human PET study show promising similarities with respect to the regional binding pattern in cerebral areas of known opioid receptor subtype composition and show the suitability of the new tracer for in vivo quantification of opioid receptor binding. Despite the less favorable (preliminary) dosimetry, the longer $t_{1/2}$ of ¹⁸F offers several advantages of this new tracer. With clinically useful applications for opioid receptor ligands emerging in pain (23) and epilepsy (4), ¹⁸F labeling makes an analog of DPN (the most established PET tracer for opiate receptor imaging) available for PET centers with no on-site cyclotron. If a PET camera is available, this tracer has advantages over the recently developed C6-O-[¹²³I]iodoallyl-DPN for SPECT (38). In addition to the better spatial resolution possible with [¹⁸F]DPN, this tracer offers the opportunity to use established models for the generation of quantitative parametric maps. Spectral analysis (30), reference tissue models (39), or the steady-state model (40) may be applied, and the estimation of VD might benefit from the opportunity to sample data for a prolonged time. The impact of the radiometabolite in the brain would require a correction for tracer kinetic modeling. One solution would be to fit a reference region for metabolism (e.g., occipital cortex) and adjust the value in the receptor region. In this case, it must be

assumed that the rate of metabolism is the same in both regions, and reference tissue models would handle the metabolite as a nonspecifically bound ligand. Such an approach might end up with unidentified SEs of the parameters and should be closely evaluated before application. A more exact approach would be to include the kinetics of the metabolite separately using a plasma input function and to adjust the metabolite rate constants. Correcting for the brain radiometabolite and using the potential of prolonged scanning would allow accurate quantification of receptor binding. In addition, it is also beneficial that DPN is a receptor antagonist and, therefore, can be used in pharmacologic doses without relevant toxicity for quantification purposes (22,26). Furthermore, as stated previously, all scientific studies with opiate receptor ligands, which require a pharmacologic or other intervention during the scanning period, can benefit from the opportunity to sample data for a prolonged period of time with [¹⁸F]DPN because signal changes induced by such an intervention become more apparent with time (21).

CONCLUSION

This study shows the feasibility and suitability of using [¹⁸F]DPN as a new PET tracer for the opioid receptor system. This human PET study revealed successful imaging of receptor binding in vivo and allowed quantification using spectral analysis. The great similarities in the pharmacokinetics and receptor binding of [¹⁸F]DPN and [¹¹C]DPN combined with the advantage of the longer $t_{1/2}$ of ¹⁸F will allow extended scanning periods, more flexible interventions (e.g., displacement studies), and DPN to be available to PET centers without an on-site cyclotron.

ACKNOWLEDGMENTS

The authors are indebted to Prof. Dr. Reingard Senekowitsch-Schmidtke and her team for carrying out the biodistribution studies; Dr. Ingo Wolf for calculating the dosimetry data; Brigitte Dzewas, Coletta Kruschke, Claudia Kolligs, Silvia Fürst, Katrin Oetjen, Dirk Wetzels, and Kai Borchers for their excellent technical assistance; and Jodi Nerve for the editorial help. The authors also thank the RDS 112 cyclotron team for the reliable routine radionuclide production. This work was supported by the Deutsche Forschungsgemeinschaft SFB 391/C9 and the Research Council of Norway (project no. 123170/320).

REFERENCES

1. Jones AKP, Cunningham VJ, Ha Kawa S, et al. Changes in central opioid receptor binding in relation to inflammation and pain in patients with rheumatoid arthritis. *Br J Rheumatol*. 1994;33:909–916.
2. Zubietta JK, Gorelick DA, Stauffer R, Ravert HT, Dannals RF, Frost JJ. Increased μ -opioid receptor binding detected by PET in cocaine-dependent men is associated with cocaine craving. *Nat Med*. 1996;2:1225–1229.
3. Burn DJ, Rinne JO, Quinn NP, Lee AJ, Marsden CD, Brooks DJ. Striatal opioid receptor binding in Parkinson's disease, striatonigral degeneration and Steele-Richardson-Olszewski syndrome: a [^{11}C]diprenorphine PET study. *Brain*. 1995;118:951–958.
4. Frost JJ, Mayberg HS, Fisher RS, et al. μ -opioid receptors measured by positron emission tomography are increased by temporal lobe epilepsy. *Ann Neurol*. 1988;23:231–237.
5. Dannals RF, Raven HT, Frost JJ, Wilson AA, Burns HD, Wagner HN Jr. Radiosynthesis of an opiate receptor binding radiotracer: [^{11}C]carfentanil. *Int J Appl Radiat Isot*. 1985;36:303–306.
6. Frost JJ, Wagner HN Jr, Dannals RF, et al. Imaging opiate receptors in the human brain by positron tomography. *J Comput Assist Tomogr*. 1985;9:231–236.
7. Lever JR, Mazza SM, Dannals RF, Ravert HT, Wilson AA, Wagner HN Jr. Facile synthesis of [^{11}C]buprenorphine for positron emission tomographic studies of opioid receptors. *Appl Radiat Isot*. 1990;41:745–752.
8. Luthra SK, Pike VW, Brady F, Horlock PL, Prenant C, Cruzel C. Preparation of [^{11}C]buprenorphine: a potential radioligand for the study of the opioid receptor system in vivo. *Appl Radiat Isot*. 1987;38:65–66.
9. Luthra SK, Brady F, Turton DR, et al. Automated radiosynthesis of [6-O-methyl- ^{11}C]diprenorphine and [6-O-methyl- ^{11}C]buprenorphine from 3-O-trityl protected precursors. *Appl Radiat Isot*. 1994;45:857–873.
10. Shiue C-Y, Bai L-Q, Teng R-R, et al. A comparison of N-(cyclopropyl[^{11}C]methyl)norbuprenorphine ([^{11}C]buprenorphine) and N-(cyclopropyl[^{11}C]methyl)nor-diprenorphine ([^{11}C]diprenorphine) in baboon using PET. *Nucl Med Biol*. 1991;18:281–288.
11. Lever JR, Schaeffel U, Kinter CM, et al. In vivo binding of N1'-([^{11}C]methyl)naltrindole to δ -opioid receptors in mouse brain. *Eur J Pharmacol*. 1992;216:459–460.
12. Frost JJ, Lever JR, Scheffer U, Dannals RF, Kinter CM, Ravert HT. Imaging delta opioid receptors in man by N11-([^{11}C]methyl)naltrindole and PET [abstract]. *J Nucl Med*. 1993;34:103P.
13. Madar I, Lever JR, Kinter CM, et al. Imaging δ -opioid receptors in human brain by N11-([^{11}C]methyl)naltrindole and PET. *Synapse*. 1996;24:19–28.
14. Pert CB, Danks JA, Channing MA, et al. 3-[^{18}F]acetylcyclofoxy: a useful probe for the visualization of opioid receptors in living animals. *FEBS Lett*. 1984;177:281–286.
15. Channing MA, Eckelman WC, Bennet JM, Burke TR, Rice KC. Radiosynthesis of [^{18}F]3-acetylcyclofoxy: a high affinity opiate antagonist. *Appl Radiat Isot*. 1985;36:429–433.
16. Cohen RM, Carson RE, Channing M, et al. F-18-cyclofoxy PET imaging in man [abstract]. *J Nucl Med*. 1988;29:796P.
17. Theodore WH, Carson RE, Andreasen P, et al. PET imaging of opiate receptor binding in human epilepsy using [^{18}F]cyclofoxy. *Epilepsy Res*. 1992;13:129–139.
18. Luthra SK, Pike VW, Brady F. The preparation of carbon-11 labelled diprenorphine: a new radioligand for the study of the opioid receptor system in vivo. *J Chem Soc Chem Commun*. 1985;1423–1425.
19. Lever JR, Dannals RF, Wilson AA, Ravert HT, Frost JJ, Wagner HN Jr. Synthesis of carbon-11 labeled diprenorphine: a radioligand for positron emission tomographic studies of opiate receptors. *Tetrahedron Lett*. 1987;28:4015–4018.
20. Luthra SK, Turton DR, Dowsett K, et al. Improved and automated radiosyntheses of [^{11}C]diprenorphine and [^{11}C]buprenorphine. *J Lab Compds Radiopharm*. 1990;30:258–259.
21. Bartenstein PA, Duncan JS, Prevett MC, et al. Investigation of the opioid system in absence seizures with positron emission tomography. *J Neurol Neurosurg Psychiatry*. 1993;56:1295–1302.
22. Jones AKP, Cunningham VJ, Ha Kawa S, et al. Quantitation of [^{11}C]diprenorphine cerebral kinetics in man acquired by PET using presaturation, pulse chase and tracer-only protocols. *J Neurosci Methods*. 1994;51:123–134.
23. Willoch F, Tölle TR, Wester HJ, et al. Central pain after pontine infarction is associated with changes in opioid receptor binding: a PET study with C-11 diprenorphine. *AJNR*. 1999;20:145–149.
24. Schadrack J, Willoch F, Platzer S, et al. Opioid receptors in human cerebellum: evidence from ^{11}C -diprenorphine PET, mRNA expression and autoradiography. *NeuroReport*. 1999;10:619–624.
25. Frost JJ, Mayberg HS, Sadzot B, et al. Comparison of [^{11}C]diprenorphine and [^{11}C]carfentanil binding to opiate receptors in humans by positron emission tomography. *J Cereb Blood Flow Metab*. 1990;10:484–492.
26. Sadzot B, Price JC, Mayberg HS, et al. Quantification of human opiate receptor concentration and affinity using high and low specific activity [^{11}C]diprenorphine and positron emission tomography. *J Cereb Blood Flow Metab*. 1991;11:204–219.
27. Bai L-Q, Teng R-R, Shiue C-Y, et al. No carrier added (NCA) N-(3-[^{18}F]fluoropropyl)-N-norbuprenorphine and N-(3-[^{18}F]fluoropropyl)-N-nordiprenorphine: synthesis, anatomical distribution in mice and rats and tomographic studies in a baboon. *Int J Appl Radiat Instrum (B)*. 1990;17:217–227.
28. Chesis PL, Hwang D-R, Welch MJ. N-(3-[^{18}F]fluoropropyl)-N-nordiprenorphine: synthesis and characterization of a new agent for imaging opioid receptors with positron emission tomography. *J Med Chem*. 1990;33:1482–1490.
29. Chesis PL, Griffith LK, Mathias CJ, Welch MJ. Sex dependent differences in N-(3-[^{18}F]fluoropropyl)-N-nordiprenorphine biodistribution and metabolism. *J Nucl Med*. 1990;31:192–201.
30. Cunningham VC, Jones T. Spectral analysis of dynamic PET studies. *J Cereb Blood Flow Metab*. 1993;13:5–23.
31. Block D, Coenen HH, Stöcklin GN. ^{18}F -fluoroalkylation of H-acidic compounds. *J Lab Compds Radiopharm*. 1987;25:201–216.
32. Stabin MG. MIRDOSE: personal computer software for internal dose assessment in nuclear medicine. *J Nucl Med*. 1996;37:538–546.
33. Cunningham VJ, Gunn RN, Byrne H, Matthews JC. Suppression of noise artifacts in spectral analysis of dynamic PET data [abstract]. *Neuroimage*. 1997;5:B72.
34. Abbott FV, Palmour RM. Morphine-6-glucuronide: analgesic effects and receptor binding profiles in rats. *Life Sci*. 1988;43:1685–1695.
35. Paternak GW, Bodnar RJ, Clark JA, Inturrisi CE. Morphine-6-glucuronide: a potent μ agonist. *Life Sci*. 1987;41:2845–2849.
36. Coenen HH, Wienhard K, Stöcklin G, et al. PET measurements of D2 and S2 receptor binding of 3-N-(2'-[^{18}F]fluoroethyl)spiperone in baboon brain. *Eur J Nucl Med*. 1988;14:80–87.
37. Moerlein SM, Perlmutter JS. Binding of 5-(2'-[^{18}F]fluoroethyl)flumazenil to central benzodiazepine receptors measured in living baboon by positron emission tomography. *Eur J Pharmacol*. 1992;218:109–115.
38. Lever JR, Ilgin S, Musachio JL, et al. Autoradiographic and SPECT imaging of central opioid receptors with iodine-123 labeled analogue of diprenorphine. *Synapse*. 1998;29:172–182.
39. Frost JJ, Douglass KH, Mayberg HS, et al. Multicompartmental analysis of [^{11}C]carfentanil binding to opiate receptors in humans measured by positron emission tomography. *J Cereb Blood Flow Metab*. 1989;9:398–409.
40. Lassen NA, Bartenstein PA, Lammertsma AA, et al. Benzodiazepine receptor quantitation in vivo in man using C-11-flumazenil and PET: application of the steady-state principle. *J Cereb Blood Flow Metab*. 1995;15:152–165.